X-ray Free Electron Lasers Motivate Bioanalytical Characterization of Protein Nanocrystals: Serial Femtosecond Crystallography

ARTICLE *in* ANALYTICAL CHEMISTRY · MARCH 2013

Impact Factor: 5.64 · DOI: 10.1021/ac303716r · Source: PubMed

1 AUTHOR:

M.J. Bogan
Stanford University
110 PUBLICATIONS **3,826** CITATIONS

analytical chemistry

Feature

pubs.acs.org/ac

X-ray Free Electron Lasers Motivate Bioanalytical Characterization of Protein Nanocrystals: Serial Femtosecond Crystallography

Atomic resolution structures of large biomacromolecular complexes can now be recorded at room temperature from crystals with submicrometer dimensions using intense femtosecond pulses delivered by the world's largest and most powerful X-ray machine, a laser called the Linac Coherent Light Source. Abundant opportunities exist for the bioanalytical sciences to help extend this revolutionary advance in structural biology to the ultimate goal of recording molecular-movies of noncrystalline biomacromolecules. This Feature will introduce the concept of serial femtosecond crystallography to the nonexpert, briefly review progress to date, and highlight some potential contributions from the analytical sciences.

Michael J. Bogan*

Stanford PULSE Institute, SLAC National Accelerator Laboratory, 2575 Sand Hill Road, Menlo Park, California 94025, United States

Supporting Information

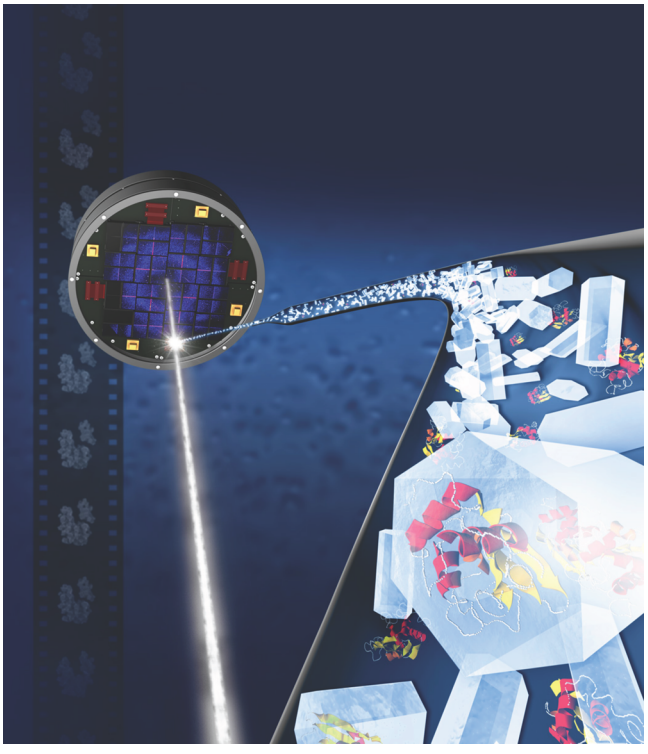

A new paradigm is emerging in structural biology, solving structures from protein *nanocrystals* at room temperature using high-intensity pulsed X-ray sources that are a billion times brighter than the newest synchrotron facilities. A global wave of investment in these new X-ray sources will open many well-defined and unforeseen opportunities in bioanalytical chemistry.

"DIFFRACTION BEFORE DESTRUCTION" X-RAY SCIENCE OPENS NEW PARADIGMS

Progress in development of X-ray sources over the last 100 years has been startling. From the first X-ray tubes to the newest synchrotron radiation facilities, the peak brightness, or roughly the number of incident X-ray photons delivered to a certain area of the sample over time, increased by about 16 orders of magnitude. The increase in brightness offered by synchrotrons facilitated advanced methods in protein crystallography, a technique leading to many Nobel Prizes including Kobilka 2012; Ramakrishnan, Steitz, and Yonath 2009; Kornberg 2006; Mackinnon 2003; and Walker 1997. In this method, target proteins are expressed and purified using bioanalytical techniques and then coerced into forming ordered crystalline structures necessary to collect X-ray diffraction data. Typically a protein crystal on the scale of tens of micrometers to millimeters is loaded onto a small mesh holder and steered into the X-ray beam. The incident X-rays scatter off the ordered proteins, and a diffraction pattern that encodes the atomic positions of the protein is recorded on an area detector. Software is used to extract this structural information, and the results are deposited in the open access Protein Data Bank, where over 85 000 structures are now stored.

The achievable resolution in protein crystallography is limited by X-ray induced radiation damage to the protein crystal.[1] This damage is both primary and secondary in nature, caused by ionization processes and radical formation. Radical diffusion can increase the extent of the damage beyond the irradiation point. To minimize the effects of damage, protein crystallography is typically performed under cryogenic conditions. However, even at low temperatures, radiation damage is a problem, especially for metalloproteins that more strongly absorb the X-ray radiation.[2]

In 2009, X-ray sources experienced another billion-fold jump in peak brightness over synchrotrons using a new technology, the hard X-ray free electron laser (XFEL).[3] The first XFEL, a U.S. Department of Energy User Facility called the Linac Coherent Light Source (LCLS), produces X-ray pulses <50 fs long with 10^{12} photons per pulse at energies between about 500 eV to 10 keV. Magaratondo and Ribic have provided a simplified

Published: March 21, 2013

   dx.doi.org/10.1021/ac303716r | *Anal. Chem.* 2013, 85, 3464−3471

description of how XFEL technology achieves these impressive and unprecedented characteristics.[4] Several reviews have described the potential applications of XFELs in structural biology, from imaging single molecules to living cells.[5−9] Hunter and Fromme have described the methods that established the use of XFELs for the structure determination of membrane-protein nanocrystals and microcrystals.[10]

XFELs offer a new "diffraction before destruction"[11,12] approach to overcome radiation damage due to the ultrafast and ultrabright nature of the X-ray pulses relative to the time scale of the damage processes.[13] If the time scale of damage is longer than the pulse duration, then the diffraction pattern represents the undamaged material. For protein crystallography, the new paradigm of "diffraction before destruction" enables a room-temperature approach called serial femtosecond crystallography (SFX).[14] Figure 1 shows a schematic of a typical SFX

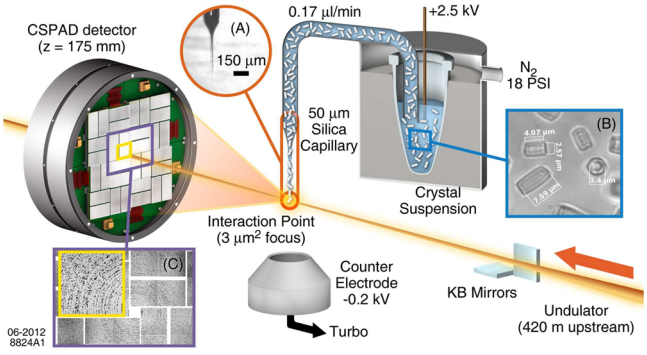

Figure 1. Serial femtosecond crystallography with X-ray lasers at the LCLS Coherent X-ray Imaging endstation. Protein structures are solved from thousands of diffraction patterns recorded from individual protein micro/nanocrystals delivered as suspensions in a thin microjet *in vacuo*. In this example, an electrospun microjet (A, scale bar 150 μm) of a thermolysin crystal suspension, (microscope image, B), flowing at 0.17 μL/min is emitted from a 50 μm i.d. silica capillary positioned <1 mm from the X-ray interaction point. An average of 2 mJ is delivered in each 40 fs pulse of 9.7 keV X-rays. Single pulse diffraction patterns from single crystals are recorded on a Cornell-SLAC Pixel Array Detector (CSPAD) positioned a distance, *z*, from the interaction region. A virtual powder pattern from 1024 LCLS shots that produced ≥16 Bragg peaks each (C) shows diffraction to <4 Å. Purple and yellow squares denote portion of CSPAD shown in the virtual powder pattern. Reproduced with permission from Sierra et al. *Acta Crystallogr. D*, **2012**, D68, 1584−1587. Copyright 2012 International Union of Crystallography (http://journals.iucr.org/).

experimental setup. Diffraction patterns from individual protein micro or nanocrystals (Figure 2) are captured one-at-a-time *before X-ray damage manifests itself.*[14] This process is repeated thousands to millions of times to record a complete data set for a single protein.

Development of the SFX technique has progressed rapidly, with demonstrations of structure determination from the lipidic sponge phase,[15] studies of the large membrane protein complex Photosystem II,[16] study of photoactivated proteins,[17] in vivo crystallization,[18] and X-ray radiation damage studies.[19,20] SFX using the Coherent X-ray Imaging (CXI) endstation[21] at the LCLS has already produced high resolution (<2 Å) protein structures,[22] including the fully glycosylated precursor complex of *Trypanosoma* brucei cysteine protease cathepsin B, a promising target for developing drugs against sleeping sickness.[23] Three years after the first LCLS experiment in 2009, AAAS recognized "X-ray Laser Advances" as a runner up to the Science

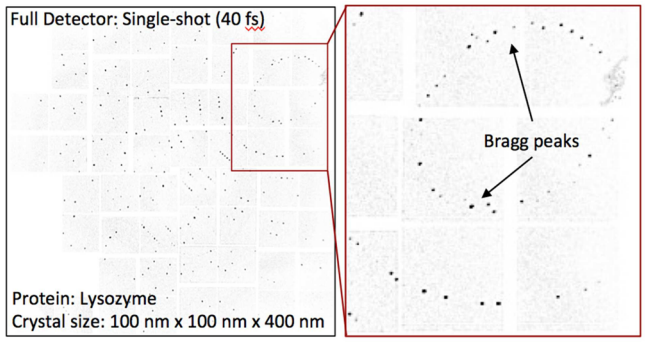

Figure 2. Background-subtracted diffraction pattern recorded from a single lysozyme crystal (100 nm ×100 nm ×400 nm) delivered into vacuum through a gas dynamic virtual nozzle and exposed to a 40 fs long, LCLS X-ray pulse with a wavelength of 1.32 Å (9.4 keV). The inset shows strong Bragg peaks (black dots) that were recorded to the edge of the detector and used to solve the structure to 1.9 Å. Many thousands of such single-shot patterns are combined to create a full data set (similar to Figure 1 C). Adapted with permission from Boutet et al. *Science* **2012**, *337*, 362−364. Copyright 2012 American Association for the Advancement of Science.

breakthrough of the year (http://www.sciencemag.org/site/special/btoy2012/index.xhtml). In early 2013, the first demonstration of simultaneous X-ray emission spectroscopy and diffraction confirmed that the electronic structure of the highly radiation-sensitive Mn_4CaO_5 cluster in the oxygen-evolving complex of Photosystem II was intact during the measurement.[24] This work opens new possibilities to solve the structure and dynamics of metal centers in metalloproteins.

SERIAL FEMTOSECOND CRYSTALLOGRAPHY DEMANDS NEW ANALYTICAL APPROACHES

The special challenges for SFX experiments include adapting to new sample delivery methods that differ from conventional protein crystallography procedures implemented at synchrotrons and instead employ liquid handling techniques more consistent with those used in the analytical sciences. Since the intense X-ray pulses destroy the sample with every shot, crystals must be replenished at 120 Hz, the LCLS repetition rate. Crystals sized 0.1−20 μm are dispersed at about 10^9 crystals/mL in aqueous solutions and are delivered from a reservoir to the X-ray interaction region through 40−100 μm internal diameter (i.d.) silica capillaries. Once the suspension arrives at the X-ray interaction region, a thin liquid jet (microjet) created at the capillary exit using gas-focusing[25] or electric fields[26] minimizes the thickness of carrier solvent surrounding the microcrystals to reduce background scattering and aid detection of the protein diffraction signal. The experiment is typically performed at $<10^{-5}$ Torr to reduce background scattering of the X-rays off of gas molecules.

Formation of the liquid microjet of protein crystal slurry in vacuo was first achieved with a gas dynamic virtual nozzle (GDVN)[25] which uses a gas sheath for flow focusing. X-rays probe the jet either within the continuous jet or at the capillary exit. The GDVN is the most extensively used liquid microjet for SFX experiments and operates at a flow rate of 10−16 μL/min.[14,15,17−20,22,23,27]

The physics of the gas and electric field flow focusing lead to comparable microjet formation,[28] suggesting that electrospray methodology would also be useful for crystal suspension delivery for SFX. A low flow rate SFX sample delivery system was

dx.doi.org/10.1021/ac303716r | *Anal. Chem.* 2013, 85, 3464−3471

developed by using the principle of electrospinning *in vacuo*,[26] where the length of the microjet at the end of the Taylor cone is extended and droplet formation is delayed by adding glycerol and/or polyethylene glycol (PEG) additives. Electrospinning is commonly used to create long nanofibers captured on a surface using an electric field applied to a liquid suspension. In the SFX application, the aim was not the end-product captured on a surface but rather to keep the crystals inside of a focused liquid stream until the X-rays probe them. The flow rate of the electrospinning microjet can be tuned from 150 nL/min to 3 μL/min by changing the silica capillary diameter and backing pressure on the sample.[26] Nanoflow electrospinning has been used for several SFX and X-ray emission spectroscopy experiments to date.[16,24,26,29] While originally designed for SFX experiments, both of these liquid microjets may find alternate utility in the analytical sciences, such as atmospheric pressure or *in vacuo* ion sources for mass spectrometry.

SFX requires delivery of billions of crystals through the liquid microjet into a 0.1−1 μm X-ray focus, one or a few crystals at a time. In current methods, overlap of crystals and X-ray pulses is random. Since the XFEL pulse is so short, the liquid jet is effectively stationary and a crystal will be exposed to the X-rays only if it resides in the interaction volume defined by the overlap of the X-ray focus and the liquid jet diameter. Weierstall and coworkers have detailed the probabilities of data acquisition in SFX.[27] Experimentally, most studies have used crystal concentrations of 10^9 to 3×10^{10} crystals per mL. A crystal "hit" is most often defined as one that produces useful, indexable, data, the typical cutoff chosen to date is 10−16 Bragg peaks. Thus, diffraction patterns with <10 are ignored and the number of diffraction patterns that must be recorded to solve a structure is larger than the number of crystals that interact with the X-rays.

More research is required to understand better the relationship between crystal dimensions experimental parameters and the probability of a creating a useful hit. To optimize SFX experiments, the number of useful diffraction patterns must be maximized while minimizing the data collection time, in effect, reducing sample consumption. Since SFX is a completely different approach for protein crystallographers that are often focused on growing the largest crystals possible, new opportunities exist in characterizing protein nanocrystals or aggregates prior to and/or during analysis with XFELs to help optimize the hit rate, probability of hitting a crystal in the microjets and probability of diffraction.

THE ANALYTE: PROTEIN NANOCRYSTALS TO SINGLE MOLECULES

Early SFX results from LCLS raise the questions: What is the size range of protein crystals suitable for SFX? How much protein is needed? How many crystals are needed? Can we define the ideal SFX experiment? What are the specific needs in analytical method development that can better inform the XFEL experiments to achieve the ideal? Can diffraction data be recorded from single molecules? A survey of published SFX data reveals insights into these questions.

No systematic SFX study of crystal size versus recorded diffraction intensity has been performed yet. Theoretical work exploring the smallest single crystal size to collect a complete data set using synchrotron crystallography placed a lower limit of 1200 nm.[30] In this paper it was noted that the lower limit would be smaller for multicrystal strategies such as XFEL studies. Powder diffraction from collections of membrane protein crystals, which contained only a few tens of unit cells and were flowing through a liquid jet, has been recorded at a synchrotron.[31] Simulations have shown that XFEL diffraction can be recorded from protein nanocrystals with a mean number of 20 molecules per side and that such data provide a new direct phasing method for solving the protein structure.[32] Indeed, experimental results have confirmed this prediction as diffraction to 1.9 Å has already been recorded from lysozyme crystals that are 100 nm × 100 nm × 400 nm on average[22] (Figure 2). The smallest known crystal to produce detectable diffraction signal with a single XFEL pulse is a 160 nm crystal of Photosystem I (PSI).[14] Photosystem I is a ∼1 MDa protein complex comprised of 36 proteins and 381 cofactors. The unit cell parameters of this crystal are $a = b = 280$ Å and $c = 165$ Å so the crystal was comprised of 5−6 complexes per side and the total number of complexes in the crystal was 125−216. Photosystem I has one of the largest unit cells of proteins in the Protein Data Bank, so it is anticipated that signal can be detected from much smaller nanocrystals, comprised of an equal number of unit cells, each with a smaller dimension. For example the unit cell dimensions of thermolysin, another protein studied by SFX,[26] are $a = b = 94$ Å and $c = 131.4$ Å. A protein crystal of 5−6 thermolysin molecules per side would be about 50−80 nm in size. Similar lysozyme crystals would be about 20−50 nm. Since diffraction has been recorded off the edge of the detectors for the 100 nm × 100 nm × 400 nm crystals (Figure 2), it is plausible that smaller crystals would still produce useful data in practice.

Knowing that SFX data can be collected from nanocrystals, which are typically ignored by protein crystallographers, except for possibly seeding growth of larger crystals, we must consider the expected size range of protein crystals that development of quantitative characterization would be valuable. The minimum dimensions of protein nanocrystals anticipated to produce data in SFX can be estimated by analyzing the unit cell dimensions for all proteins in the Protein Data Bank. Assuming that signal can be detected from crystals with dimensions similar to the smallest recorded in SFX experiments to-date, about 10 × 10 × 10 unit cells, we find that the most systems will fall in the size range of 25−500 nm (Figure 3).

To provide insight into how much protein is necessary to perform an SFX experiment, data from all published experiments

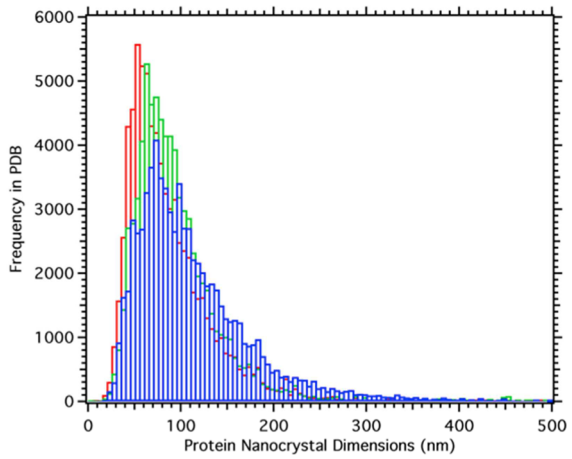

Figure 3. Projected minimum protein nanocrystal dimensions suitable for SFX range from 25 to 500 nm, based on 10 × 10 × 10 unit cells. Each unit cell dimension *a*, *b*, or *c* is plotted separately in red, green, or blue, respectively. Data is calculated from a histogram of crystal unit cell dimensions in the Protein Data Bank (PDB).

dx.doi.org/10.1021/ac303716r | *Anal. Chem.* 2013, 85, 3464−3471

is summarized in Figure 4. In all experiments, the total number of crystal patterns recorded, with ≥10 or 16 Bragg peaks, is reported

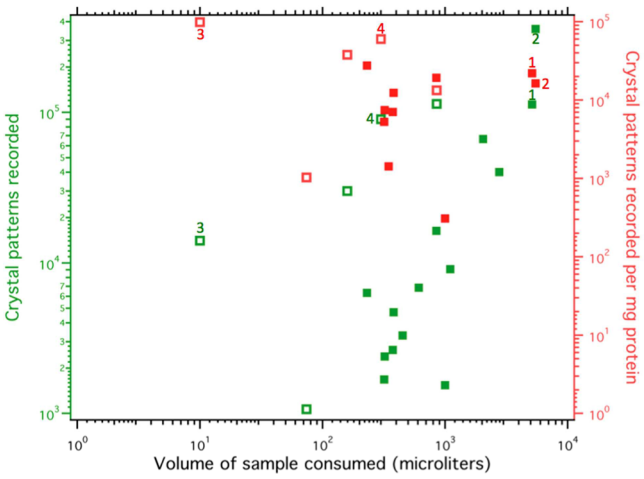

Figure 4. Summary of published SFX data to date: A plot of the single-shot crystal diffraction patterns (≥10−16 Bragg peaks) recorded in total (green) and per milligram of protein consumed (red), for the GDVN (solid) and electrospinning (open) jets, as a function of total sample volume consumed displays the relative efficiency of various SFX experiments.

in the manuscript. The volume of sample consumed for all SFX experiments has ranged from 10 μL to 5500 μL and protein concentrations are 1−22 mg/mL. By relating the total number of crystal diffraction patterns collected per milligram of protein consumed with the sample volume consumed, the relative efficiency of experiments can be compared.

Four sets of data points will be compared for this discussion. Point 1 is the first SFX experiment ever performed.[14] A large sample volume was consumed because the required number of diffraction patterns necessary to solve the protein structure was unknown. The experimental aim, in this case, was to record as much data as possible. Point 2 is a recent experiment, solution of a previously unsolved protein structure, a fully glycosylated precursor complex of *Trypanosoma* brucei cysteine protease cathepsin B (catB).[23] Again, a large volume of sample was consumed to ensure a sufficiently large data set, since no unknown structure had been solved by an XFEL yet. The difference between the first and most recently reported experiments is clear, even though the diffraction patterns (with ≥10 Bragg peaks) collected per milligram of protein was 35% higher in the first experiment, the total number of diffraction patterns recorded for catB was 3 times higher. For point 3, the electric-field focused microjet based on electrospinning, operating at 170 nL/min, was used to collect data from thermolysin crystals.[26] In this case, only 10 μL of sample was consumed but ∼10^5 diffraction patterns or 4−6 times higher than points 1 and 2 was recorded, even with a more stringent constraint of ≥16 Bragg peaks applied to the data. Point 4 is data collected from the large membrane protein complex Photosystem II using the electrospinning microjet,[24] demonstrating that high diffraction per mg can be recorded for large multiprotein complexes as well. A tabulated version of the data, including sample flow rate and the resolution of the solved structure for each experiment is available in the Supporting Information.

It is difficult to directly compare the differences in the various SFX experiments because of the small number of experiments, the wide array experimental parameters, and the different biophysical properties of the protein crystals themselves. However, plots such as Figure 4 will help identify successful optimization efforts. One of the keys in increasing the efficiency of experiments using a gas-focused liquid jet[25] was the development of a rotating syringe pump to mitigate settling of the protein crystals.[33] This device may prove useful for other analytical techniques aiming to study nanoparticle suspensions that are sensitive to sonication. As mentioned earlier, better understanding of the probability of recording useful diffraction for various protein crystal preparations will help optimize SFX experiments to achieve ideal conditions.

Discussion of differences between the two injection systems and opportunities for improvements is useful to guide future development. Weierstall and co-workers have extensively detailed the advantages, disadvantages, and opportunities for further development of the GDVN.[27] A key improvement for the GDVN would be the reproducibility of the nozzle design, which is being actively pursued using microfluidic chip designs. The electric-field focused jet design minimizes clogging issues two ways: (1) by using a larger 75 or 100 μm inner diameter capillary while still achieving a ∼1 μL/min or 3 μL/min flow rate, respectively, and (2) it uses no unions or inline filters so the propensity for clogging at interfaces and junctions between connectors is eliminated. The lack of need for a sheath gas flow for the electric field focused jet means that it easily operates at <10^{-5} Torr without differential pumping. This creates an open geometry that enables experiments such as the first simultaneous X-ray emission spectroscopy and diffraction from Photosystem II that proved the electronic structure of the metal center is intact during the measurement.[24] The main drawbacks of the electric-field focused jet are that the low flow rate increases the length of time for the liquid to reach the end of the capillary (the distance from the sample reservoir to the interaction region is 1 m), and the unionless design means that sample changes introduce air bubbles that can destabilize the jet. The first issue can be overcome by applying higher pressure on the sample reservoir to increase sample flow rate temporarily or by shortening the distance to the interaction region, and the second issue can be overcome by providing a sample reloading mechanism that does not require a union, such as refilling the sample reservoir via a needle through a septum.

DEFINING AN IDEAL SFX EXPERIMENT?

Figure 4 also gives us insight into how far we are from the ideal experiment. Diffraction strength is dependent on the number of unit cells in the crystal, the number of proteins in the repeating symmetry unit, and identical nature of each unit cell. We expect protein crystals with 10 × 10 × 10 unit cells, irrespective of protein molecular weight, will give sufficient signal from an XFEL pulse with a 1 μm^2 or smaller focus. For lysozyme, the first protein simulated for single particle diffraction with XFELs[13] and the first high resolution structure solved with XFELs,[22] the total mass per 10 × 10 × 10 crystal is 0.02 fg. If we assume a 100% hit rate and no wasted sample, 0.5 pg would be consumed to record 25 000 diffraction patterns, or 5 × 10^{13} crystal patterns per mg. As the molecular weight of the protein increases, the expected crystal patterns per mg decreases, e.g. for thermolysin or a MDa protein complex like PSI, 2 × 10^{13} and 6 × 10^{11} crystal patterns per mg, respectively. The most efficient experiment to date

dx.doi.org/10.1021/ac303716r | *Anal. Chem.* 2013, 85, 3464−3471

(point 3, Figure 4) is about 7 orders of magnitude below this value.

The large discrepancy between the ideal experiment described above and the experiments published to date can be mainly explained with two parameters, protein crystal size polydispersity and the random arrival of the crystals to the X-ray interaction region. Since the crystals are not tuned to exactly 10 × 10 × 10 unit cells, or whatever the optimal size turns out to be, any larger crystals in the slurry consume more mass per diffraction pattern. The random distribution of the crystals inside the liquid jet means that the majority of crystals pass through the interaction region without ever being exposed to the X-rays, due to the 8.3 ms time delay between each of the LCLS X-ray pulses. Since the laser pulse is only about 50 fs long, essentially the entire sample is unexposed. Improving the size monodispersity of crystals and timing individual crystal delivery to individual X-ray pulses would greatly enhance the SFX experiment efficiency. A gain in the crystal patterns recorded per mg will also be achieved when higher repetition rate XFEL facilities are available. XFEL repetition rate is projected to provide at least an order of magnitude more efficiency. For example, the European XFEL is projected to produce 27 000 pulses per second. Early detectors are expected to record 3 000 pulses per second, resulting in a potential efficiency gain of 25 over the 120 Hz operation of LCLS; later detectors will result in even more efficiency gains.

■ ANALYTICAL METHOD DEVELOPMENT IN SFX

Although it is known that efforts to prepare more monodisperse crystal sizes would improve experimental efficiency, the ideal number of unit cells to collect data for SFX is still unknown. Thus SFX studies of diffraction quality versus crystal size are warranted. Analytical separations technology should be employed to prepare and concentrate the various size batches, for example, the separation of protein nanocrystals (about 25−500 nm as defined above) from microcrystals. Overall, it is anticipated that SFX will be particularly suitable to large multimeric protein complexes and membrane proteins not amenable to large crystal growth so techniques geared toward the larger end of the size range in Figure 3 may prove particularly valuable. Analytical ultracentrifugation on microvolumes will also be valuable. Multiphase separations demonstrated for inorganic nanoparticles of various sizes[34] could be adapted for protein nanocrystals. It is known that well-diffracting nanocrystals can be formed by crushing microcrystals using a mortar and pestle or bead-based methods,[18,23] so analytical methods can be developed using nanocrystals generated from grinding of larger crystals. It should be possible to develop a set of standard protein nanocrystals, even using commercially available samples such as glucose isomerase microcrystal suspensions (Hampton Research) that would be useful for characterizing the different methods developed.

To optimize separation methods, crystal growth, or production of nanocrystals from grinding, it is necessary to count the number of protein crystals in microliter volumes of complex solvent systems. Quantitating the number of crystals per sample volume is a pressing need, and several existing analytical tools designed to characterize protein aggregates and nanoparticles, such as nanoparticle tracking analysis,[35] should be explored. In this method, a laser shines through a liquid suspension of particles and a video of the resulting scattering is recorded. Software is then used to measure the particle diffusion due to Brownian motion, correlating particle size through the Stokes−Einstein relationship, and calculating a particle density based on the number of tracked objects found in the known volume. Light scattering methods can determine particle size but cannot distinguish sample crystallinity. Second order nonlinear optical imaging of chiral crystals (SONNIC) is an emerging method capable of identifying membrane protein crystals, even in challenging opaque or turbid environments such as lipid cubic phases.[36]

The unique ability of SFX to study nanocrystals in flowing streams opens the possibility to study the diffusion of substrates into protein nanocrystals in real-time, to quantitatively record molecular movies of protein−substrate complexes in defined states. Thus methods focused on tracking flowing nanocrystals or quantifying substrate uptake into protein nanocrystals will be valuable. Development of liquid microjets compatible with mixing experiments will also be important and very elegant designs for gas-focused jets have already been reported.[27] Electric-field focused jets could benefit from applying coaxial capillary strategies used in time-resolved electrospray mass spectrometry studies.[37] Coaxial electrospray experiments, where the inner capillary can be moved to change the mixing time, should easily adapt to electrospinning *in vacuo*.

■ MASS SPECTROMETER-BASED BIOMOLECULAR ION DELIVERY TO XFELS FOR SINGLE MOLECULE DIFFRACTION

XFELs may one day help solve the structure of gas phase protein ions. XFEL pulses are so intense that individual noncrystalline samples such as viruses[38] or airborne particulate matter in flight[39] can currently be imaged to nanometer resolution. Using this single particle diffractive imaging[40] experiment with a submicrometer focused XFEL and assembling multiple single shots of randomly oriented particles[41,42] could enable imaging of single molecules.[13] Now that many of the critical milestones in "diffraction before destruction" X-ray science have been achieved, including single particle structure determination from single-shot diffraction patterns of individual nanoparticles,[41,42] we are closer than ever to molecular imaging with XFEL's.[43]

Electrospray mass spectrometry methods were recognized as a potential method to deliver single molecules into X-ray laser pulses, even before XFEL facilities existed.[13] Electrospray has been used in conjunction with customized digital ion trap technology to study biomolecules by small-angle X-ray scattering with synchrotrons.[44] The number of molecules a 3D trap can hold, or loading capacity, is limited by the space charge effect because the ion cloud is cooled with He gas and trapped in the center. This effect likely renders the ion population density insufficient for single molecule imaging with XFELs.

It would be advantageous to develop protein ion bunching technology for use in X-ray scattering experiments. Sample delivery to a 100 nm focused XFEL has very stringent requirements. One molecule in a 0.1 × 0.1 × 100 = 1 μm^3 X-ray interaction region (at a specific time) corresponds to 10^{12} ions/cm^3. To produce such high charge densities in the X-ray interaction region, ions must be bunched together on short time scales, overcoming space charge limitations. For example, the C-trap technology developed for use in orbitrap mass spectrometers[45] seems particularly suitable to the study of gas phase biomolecular ions with XFELs. A recent report of orbitrap analysis of large macromolecular complexes like the 801 kDa GroEL,[46] one of the systems simulated for single molecule imaging,[47] increases the potential for crossover of this technology to experiments with XFELs. The orbitrap has stringent requirements on ion packet injection for its high-resolution

dx.doi.org/10.1021/ac303716r | *Anal. Chem.* 2013, 85, 3464−3471

operation. Ion packets must be injected with durations much shorter than one axial oscillation in the orbitrap to ensure coherent motion. The C-trap can deliver about 5×10^5 charges into roughly 10^7 μm^3, or 0.05 e/μm^3. Assuming an X-ray focus with a 1 μm^3 sample volume and GroEL in the 70^+ charge state (m/z ~11 400), this translates to only about 0.004 GroEL molecules per pulse. It is possible that custom modifications designed for XFEL experiments may provide an order of magnitude increase in molecular ion density. Optimization of the mass-to-charge selected ion packet delivery to the XFEL submicrometer focus could potentially resolve the long-standing question of the structure of gas phase biomolecular ions.

GLOBAL INVESTMENT IN XFEL FACILITIES IS GROWING

The demand for analytical methods associated with XFEL research is anticipated to grow quickly. Many countries around the world are actively pursuing development of XFEL facilities.[48] Figure 5 shows the minimum anticipated worldwide capacity for

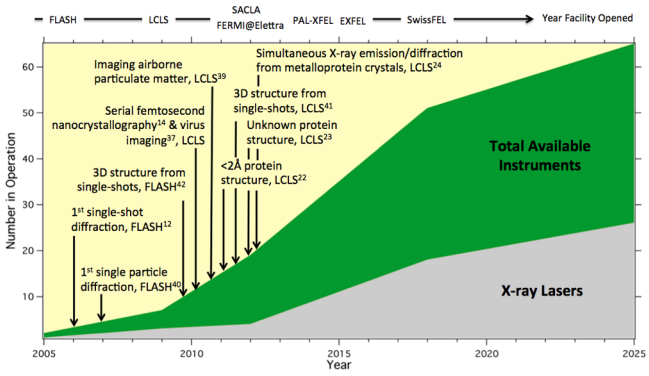

Figure 5. Projected worldwide capacity for X-ray free electron laser facilities. Several milestones in single particle diffraction and serial femtosecond crystallography are noted. The approximate dates of the XFEL facility opening are listed at the top.

XFEL user endstations by 2025. The Japanese user facility SACLA opened in 2012, and by 2017, both the European XFEL and the SwissFEL should be operational.

Over time, a synergy will develop between the demanding new protein nanocrystal experiments and the bioanalytical tools to characterize the nanocrystals to single molecules. The technologies developed for XFEL research such as liquid microjets or microfluidic chips could be applied to traditional bioanalytical methods like mass spectrometry or other capillary flowing techniques. The ultrafast and ultrabright X-ray pulses from XFELs may also find analytical utility themselves. Synchrotron-based hydroxyl radical footprinting mass spectrometry has proven a useful analytical tool to probe dynamic protein structures and interfaces.[49] XFEL radiolysis may find unique applications due to the pulsed, high intensity and narrowly focused nature of the radiation. Opportunities also exist for analytical methods based on XFEL X-ray emission spectroscopy, which has proven highly sensitive. To create a $K\beta_{1,3}$ X-ray emission spectrum from PSII crystals, an estimated sample volume of 0.3 nL or a total of 2 pmol of Mn was analyzed.[24] Now that "diffraction before destruction" has been proven valid, the development of bioanalytical methods for sample characterization, mounting, or injection coupled to XFEL facility growth will rapidly increase basic research discoveries and their application to challenging scientific problems.

ASSOCIATED CONTENT

Supporting Information

Table summarizing data of published serial femtosecond crystallography experiments used to generate Figure 4. This material is available free of charge via the Internet at http://pubs.acs.org.

AUTHOR INFORMATION

Corresponding Author

*E-mail: mbogan@slac.stanford.edu.

Notes

The authors declare no competing financial interest.

Biography

Michael J. Bogan is a Staff Scientist at the Stanford PULSE Institute, SLAC National Accelerator Laboratory. He completed his Ph.D. in Chemistry under the guidance of Prof. George R. Agnes at Simon Fraser University. As a 2004 NSERC postdoctoral fellow, he joined two research teams at the Lawrence Livermore National Laboratory: one developing single particle aerosol mass spectrometry methods (Matthias Frank) and the other building the first single pulse imaging experiments to be performed with an X-ray free electron laser (Henry Chapman). Since joining SLAC in 2008, he leads a research group that develops biological sample delivery methods to X-ray free electron lasers (XFELs). Of particular interest are methods to reduce sample consumption of precious biological samples to perform protein crystallography or single virus particle analysis. His group also leads research, as part of a large international collaboration, exploring XFEL imaging of airborne particulate matter (PM2.5) to nanometer resolution.

ACKNOWLEDGMENTS

This work was supported by the AMOS program, Office of Science, Office of Basic Energy Sciences (OBES), Division of Chemical Sciences, Geosciences, and Biosciences (CSGB) of the Department of Energy (DOE) and through the SLAC Laboratory Directed Research and Development Program. LCLS is a national user facility operated by Stanford University on behalf of the U.S. Department of Energy (DOE), Office of Basic Energy Sciences. The author acknowledges helpful discussions with Alexander Makarov regarding the C-trap and Greg Stewart for the cover artwork.

REFERENCES

(1) Henderson, R. *Q. Rev. Biophys.* **1995**, *144*, 171−193.

(2) Yano, J.; Kern, J.; Irrgang, K.-D.; Latimer, M. J.; Bergmann, U.; Glatzel, P.; Pushkar, Y.; Biesiadka, J.; Loll, B.; Sauer, K.; Messinger, J.; Zouni, A.; Yachandra, V. K. *Proc. Natl. Acad. Sci. U.S.A.* **2005**, *102*, 12047−12052.

(3) Emma, P.; Akre, R.; Arthur, J.; Bionta, R.; Bostedt, C.; Bozek, J.; Brachmann, A.; Bucksbaum, P.; Coffee, R.; Decker, F. J.; Ding, Y.; Dowell, D.; Edstrom, S.; Fisher, A.; Frisch, J.; Gilevich, S.; Hastings, J.; Hays, G.; Hering, P.; Huang, Z.; Iverson, R.; Loos, H.; Messerschmidt, M.; Miahnahri, A.; Moeller, S.; Nuhn, H. D.; Pile, G.; Ratner, D.; Rzepiela, J.; Schultz, D.; Smith, T.; Stefan, P.; Tompkins, H.; Turner, J.; Welch, J.; White, W.; Wu, J.; Yocky, G.; Galayda, J. *Nat. Photon.* **2010**, *4*, 641−647.

(4) Margaritondo, G.; Ribic, P. R. *J. Synchrotron Rad.* **2011**, *18*, 101−108.

(5) Schlichting, I.; Miao, J. *Curr. Opin. Struct. Biol.* **2012**, *22*, 613−626.

(6) Bergh, M.; Huldt, G.; Timneanu, N.; Maia, F. R. N. C.; Hajdu, J. *Q. Rev. Biophys.* **2008**, *41*, 181−204.

(7) Spence, J. C. H.; Weierstall, U.; Chapman, H. N. *Rep. Prog. Phys.* **2012**, *75*, 102601.

(8) Gaffney, K. J.; Chapman, H. N. *Science* **2007**, *316*, 1444−1448.
(9) Miao, J.; Chapman, H. N.; Kirz, J.; Sayre, D.; Hodgson, K. O. *Annu. Rev. Biophys. Biomol. Struct.* **2004**, *33*, 157−176.
(10) Hunter, M. S.; Fromme, P. *Methods* **2011**, *55*, 387−404.
(11) Spence, J. C.; Hawkes, P. W. *Ultramicroscopy* **2008**, *108*, 1502−1503.
(12) Chapman, H. N.; Barty, A.; Bogan, M. J.; Boutet, S.; Frank, M.; Hau-Riege, S. P.; Marchesini, S.; Woods, B. W.; Bajt, S.; Benner, W. H.; London, R. A.; Plonjes, E.; Kulmann, M.; Treusch, R.; Dusterer, S.; Tschentscher, T.; Schneider, J. R.; Spiller, E.; Moller, T.; Bostedt, C.; Hoener, M.; Shapiro, D. A.; Hodgson, K. O.; van der Spoel, D.; Burmeister, F.; Bergh, M.; Caleman, C.; Huldt, G.; Seibert, M. M.; Maia, F. R. N. C.; Lee, R. W.; Szoke, A.; Timneanu, N.; Hajdu, J. *Nat. Phys.* **2006**, *2*, 839−843.
(13) Neutze, R.; Wouts, R.; van der Spoel, D.; Weckert, E.; Hajdu, J. *Nature* **2000**, *406*, 752−757.
(14) Chapman, H.; Fromme, P.; Barty, A.; White, T.; Kirian, R.; Aquila, A.; Hunter, M.; Schulz, J.; Deponte, D.; Weierstall, U.; Doak, B.; Maia, F.; Martin, A.; Schlichting, I.; Lomb, L.; Coppola, N.; Shoeman, R.; Epp, S. W.; Hartman, R. L.; Rolles, D.; Rudenko, A.; Foucar, L.; Kimmel, N.; Weidenspointner, G.; Holl, P.; Liang, M.; Barthelmess, M.; Caleman, C.; Boutet, S.; Bogan, M. J.; Kryzwinski, J.; Bostedt, C.; Bajt, S.; Gumprecht, L.; Rudek, B.; Erk, B.; Schmidt, C.; Homke, A.; Reich, C.; Pietschner, D.; Struder, L.; Hauser, G.; Gorke, H.; Ullrich, J.; Herrmann, S.; Schaller, G.; Schopper, F.; Soltau, H.; Kuhnel, K. U.; Messerschmidt, M.; Bozek, J. D.; Hau-Riege, S. P.; Frank, M.; Hampton, C. Y.; Sierra, R. G.; Starodub, D.; Williams, G.; Hajdu, J.; Timneanu, N.; Seibert, M. M.; Andreasson, J.; Rocker, A.; Jonsson, O.; Stern, S.; Nass, K.; Andritschke, R.; Schroter, C. D.; Frasniqi, F.; Bott, M.; Schmidt, K.; Wang, X.; Grotjohann, I.; Holton, J.; Marchesini, S.; Schorb, S.; Rupp, D.; Adolph, M.; Gorkhover, T.; Hirsemann, H.; Potdevin, G.; Graafsma, H.; Nilsson, B.; Spence, J. C. H. *Nature* **2011**, *470*, 73−77.
(15) Johansson, L. C.; Arnlund, D.; White, T. A.; Katona, G.; Deponte, D.; Weierstall, U.; Doak, R. B.; Shoeman, R. L.; Lomb, L.; Malmerberg, E.; Davidsson, J.; Nass, K.; Liang, M.; Andreasson, J.; Aquila, A.; Bajt, S.; Barthelmess, M.; Barty, A.; Bogan, M. J.; Bostedt, C.; Bozek, J.; Caleman, C.; Coffee, R.; Coppola, N.; Ekeberg, T.; Epp, S. W.; Erk, B.; Fleckenstein, H.; Foucar, L.; Fromme, P.; Graafsma, H.; Gumprecht, L.; Hajdu, J.; Hampton, C. Y.; Hartmann, R.; Hartmann, A.; Hauser, G.; Hirsemann, H.; Holl, P.; Holton, J.; Hunter, M. S.; Kassemeyer, S.; Kimmel, N.; Kirian, R.; Maia, F. N. C.; Marchesini, S.; Martin, A. V.; Reich, C.; Rolles, D.; Rudek, B.; Rudenko, A.; Schlichting, I.; Schulz, A.; Seibert, M. M.; Sierra, R. G.; Soltau, H.; Starodub, D.; Stellato, F.; Stern, E. S.; Struder, L.; Timneanu, N.; Ullrich, J.; Wang, X.; Weidenspointer, G.; Wunderer, C.; Chapman, H. N.; Spence, J. C. H.; Neutze, R. *Nat. Methods* **2012**, *9*, 263−265.
(16) Kern, J.; Alonso-Mori, R.; Hellmich, J.; Tran, R.; Hattne, J.; Laksmono, H.; Glockner, C.; Echols, N.; Sierra, R. G.; Sellberg, J.; Lassalle-Kaiser, B.; Gildea, R. J.; Glatzel, P.; Grosse-Kunstleve, R. W.; Latimer, M. J.; McQueen, T. A.; DiFiore, D.; Fry, A. R.; Messerschmidt, M.; Miahnahri, A.; Schafer, D. W.; Seibert, M. M.; Sokaras, D.; Weng, T.-C.; Zwart, P. H.; White, W. E.; Adams, P. D.; Bogan, M. J.; Boutet, S.; Williams, G. J.; Messinger, J.; Sauter, N. K.; Zouni, A.; Bergmann, U.; Yano, J.; Yachandra, V. K. *Proc. Nat. Acad. Sci. U.S.A.* **2012**, *109*, 9721−9726.
(17) Aquila, A.; Hunter, M. S.; Doak, R. B.; Kirian, R. A.; Fromme, P.; White, T. A.; Andreasson, J.; Arnlund, D.; Bajt, S.; Barends, T. R. M.; Barthelmess, M.; Bogan, M. J.; Bostedt, C.; Bottin, H.; Bozek, J. D.; Caleman, C.; Coppola, N.; Davidsson, J.; Deponte, D.; Elser, V.; Epp, S. W.; Erk, B.; Fleckenstein, H.; Foucar, L.; Frank, F.; Fromme, R.; Graafsma, H.; Grotjohann, I.; Gumprecht, L.; Hajdu, J.; Hampton, C. Y.; Hartmann, A.; Hartmann, R.; Hau-Riege, S. P.; Hauser, G.; Hirsemann, H.; Holl, P.; Holton, J. M.; Homke, A.; Johansson, L.; Kimmel, N.; Kassemeyer, S.; Krasniqi, F.; Kuhnel, K. U.; Liang, M.; Lomb, L.; Malmerberg, E.; Marchesini, S.; Martin, A. V.; Maia, F. R. N. C.; Messerschmidt, M.; Nass, K.; Reich, C.; Neutze, R.; Rolles, D.; Rudek, B.; Rudenko, A.; Schlichting, I.; Schmidt, C.; Schmidt, K. E.; Schulz, J.; Seibert, M. M.; Shoeman, R. L.; Sierra, R. G.; Soltau, H.; Starodub, D.; Stellato, F.; Stern, S.; Struder, L.; Timneanu, N.; Ullrich, J.; Wang, X.; Williams, G.; Weidenspointer, G.; Weierstall, U.; Wunderer, C.; Barty, A.; Spence, J. C. H.; Chapman, H. N. *Opt. Express* **2012**, *20*, 2706−2716.
(18) Koopmann, R.; Cupelli, K.; Redecke, L.; Nass, K.; Deponte, D.; White, T. A.; Stellato, F.; Rehders, D.; Liang, M.; Andreasson, J.; Aquila, A.; Bajt, S.; Barthelmess, M.; Barty, A.; Bogan, M. J.; Bostedt, C.; Bozek, J.; Caleman, C.; Coppola, N.; Davidsson, J.; Doak, B.; Ekeberg, T.; Epp, S.; Erk, B.; Fleckenstein, H.; Foucar, L.; Graafsma, H.; Gumprecht, L.; Hajdu, J.; Hampton, C. Y.; Hanrtmann, A.; Hartmann, R.; Hauser, G.; Hirsemann, H.; Holl, P.; Hunter, M. S.; Kassemeyer, S.; Kimmel, N.; Kirian, R.; Lomb, L.; Maia, F. R. N. C.; Martin, A. V.; Messerschmidt, M.; Reich, C.; Rolles, D.; Rudek, B.; Rudenko, A.; Schlichting, I.; Schulz, J.; Seibert, M. M.; Shoeman, R. L.; Sierra, R. G.; Soltau, H.; Stern, S.; Struder, L.; Timneanu, N.; Ullrich, J.; Wang, X.; Weidenspointer, G.; Weierstall, U.; Williams, G. J.; Wunderer, C.; Fromme, P.; Spence, J. C. H.; Stehle, T.; Chapman, H. N.; Betzel, C.; Duszenko, M. *Nat. Methods* **2012**, *9*, 259−262.
(19) Lomb, L.; Barends, T.; Kassemeyer, S.; Aquila, A.; Epp, S. W.; Erk, B.; Foucar, L.; Hartmann, R.; Rudek, B.; Rolles, D.; Rudenko, A.; Shoeman, R. L.; Andreasson, J.; Bajt, S.; Barthelmess, M.; Barty, A.; Bogan, M. J.; Bostedt, C.; Bozek, J. D.; Caleman, C.; Coffee, R.; Coppola, N.; DePonte, D. P.; Doak, R. B.; Ekeberg, T.; Fleckenstein, H.; Fromme, P.; Gebhardt, M.; Graafsma, H.; Gumprecht, L.; Hajdu, J.; Hampton, C. Y.; Hartmann, A.; Hauser, G.; Hirsemann, H.; Holl, P.; Holton, J.; Hunter, M. S.; Kabsch, W.; Kimmel, N.; Kirian, R. A.; Liang, M.; Maia, F. R. N. C.; Meinhart, A.; Marchesini, S.; Martin, A. V.; Nass, K.; Reich, C.; Schulz, J.; Seibert, M. M.; Sierra, R. G.; Soltau, H.; Spence, J. C. H.; Steinbrener, J.; Stellato, F.; Stern, S.; Timneanu, N.; Wang, X.; Weidenspointner, G.; Weierstall, U.; White, T. A.; Wunderer, C.; Chapman, H. N.; Ullrich, J.; Struder, L.; Schlichting, I. *Phys. Rev. B* **2011**, *84*, 214111.
(20) Barty, A.; Caleman, C.; Aquila, A.; Timneanu, N.; Lomb, L.; White, T. A.; Andreasson, J.; Arnlund, D.; Bajt, S.; Barends, T.; Barthelmess, M.; Bogan, M. J.; Bostedt, C.; Bozek, J. D.; Coffee, R.; Coppola, N.; Davidson, J.; DePonte, D. P.; Doak, R. B.; Ekeberg, T.; Elser, V.; Epp, S. W.; Erk, B.; Fleckenstein, H.; Foucar, L.; Fromme, P.; Graafsma, H.; Gumprecht, L.; Hajdu, J.; Hampton, C. Y.; Hartmann, R.; Hartmann, A.; Hauser, G.; Hirsemann, H.; Holl, P.; Hunter, M. S.; Johansson, L.; Kassemeyer, S.; Kimmel, N.; Kirian, R. A.; Liang, M.; Maia, F. R. N. C.; Malmerberg, E.; Marchesini, S.; Martin, A. V.; Nass, K.; Neutze, R.; Reich, C.; Rolles, D.; Rudek, B.; Rudenko, A.; Scott, H.; Schlichting, I.; Schulz, J.; Seibert, M. M.; Shoeman, R. L.; Sierra, R. G.; Soltau, H.; Spence, J. C. H.; Stellato, F.; Stern, S.; Struder, L.; Ullrich, J.; Wang, X.; Weidenspointer, G.; Weierstall, U.; Wunderer, C.; Chapman, H. N. *Nat. Photon.* **2011**, *6*, 35−40.
(21) Boutet, S.; Williams, G. *New J. Phys.* **2010**, *12*, 035024.
(22) Boutet, S.; Lomb, L.; Williams, G. J.; Barends, T. R. M.; Aquila, A.; Doak, R. B.; Weierstall, U.; Deponte, D.; Steinbrener, J.; Shoeman, R. L.; Messerschmidt, M.; Barty, A.; White, T. A.; Kassemeyer, S.; Kirian, R.; Seibert, M. M.; Montanez, P.; Kenney, C.; Herbst, R.; Hart, P.; Pines, J.; Haller, G.; Gruner, S. M.; Philipp, H. T.; Tate, M. W.; Hromalik, M.; Koerner, L. J.; van Bakel, N.; Morse, J.; Ghonsalves, W.; Arnlund, D.; Bogan, M. J.; Caleman, C.; Fromme, R.; Hampton, C. Y.; Hunter, M. S.; Johansson, L.; Katona, G.; Kupitz, C.; Liang, M.; Martin, A. V.; Nass, K.; Redecke, L.; Stellato, F.; Timneanu, N.; Wang, D.; Zatepsin, N.; Schafer, D.; Defever, J.; Neutze, R.; Fromme, P.; Spence, J. C. H.; Chapman, H. N.; Schlichting, I. *Science* **2012**, *337*, 362−364.
(23) Redecke, L.; Nass, K.; DePonte, D. P.; White, T. A.; Rehders, D.; Barty, A.; Stellato, F.; Liang, M.; Barends, T. R. M.; Boutet, S. b.; Williams, G. J.; Messerschmidt, M.; Seibert, M. M.; Aquila, A.; Arnlund, D.; Bajt, S.; Barth, T.; Bogan, M. J.; Caleman, C.; Chao, T.-C.; Doak, R. B.; Fleckenstein, H.; Frank, M.; Fromme, R.; Galli, L.; Grotjohann, I.; Hunter, M. S.; Johansson, L. C.; Kassemeyer, S.; Katona, G.; Kirian, R. A.; Koopmann, R.; Kupitz, C.; Lomb, L.; Martin, A. V.; Mogk, S.; Neutze, R.; Shoeman, R. L.; Steinbrener, J.; Timneanu, N.; Wang, D.; Weierstall, U.; Zatsepin, N. A.; Spence, J. C. H.; Fromme, P.; Schlichting, I.; Duszenko, M.; Betzel, C.; Chapman, H. N. *Science* **2013**, *339*, 227−230.
(24) Kern, J.; Alonso-Mori, R.; Tran, R.; Hattne, J.; Gildea, R. J.; Echols, N.; Gloeckner, C.; Hellmich, J.; Laksmono, H.; Sierra, R. G.;

Lassalle-Kaiser, B.; Koroidov, S.; Lampe, A.; Han, G.; Gul, S.; DiFiore, D. r.; Milathianaki, D.; Fry, A. R.; Miahnahri, A.; Schafer, D. W.; Messerschmidt, M.; Seibert, M. M.; Koglin, J. E.; Sokaras, D.; Weng, T.-C.; Sellberg, J.; Latimer, M. J.; Grosse-Kunstleve, R. W.; Zwart, P. H.; White, W. E.; Glatzel, P.; Adams, P. D.; Bogan, M. J.; Williams, G. J.; Boutet, S. b.; Messinger, J.; Zouni, A.; Sauter, N. K.; Yachandra, V. K.; Bergmann, U.; Yano, J. *Science* **2013**, DOI: 10.1126/science.1234273.

(25) DePonte, D. P.; Weierstall, U.; Schmidt, K.; Warner, J.; Starodub, D.; Spence, J. C. H.; Doak, R. B. *J. Phys. D: Appl. Phys.* **2008**, *41*, 195505.

(26) Sierra, R. G.; Laksmono, H.; Kern, J.; Hattne, J.; Alonso-Mori, R.; Gloeckner, C.; Tran, R.; Hellmich, J.; Lassalle-Kaiser, B.; Schafer, D. W.; Sellberg, J.; McQueen, T. A.; Fry, A.; Messerschmidt, M.; Miahnahri, A.; Seibert, M. M.; Hampton, C. Y.; Starodub, D.; Loh, N. T. D.; Zwart, P. H.; Milathianaki, D.; White, W. E.; Adam, P. D.; Boutet, S.; Williams, G. J.; Messinger, J.; Sauter, N. K.; Zouni, A.; Bergmann, U.; Yano, J.; Yachandra, V. K.; Bogan, M. J. *Acta Cryst. D* **2012**, *D68*, 1584−1587.

(27) Weierstall, U.; Spence, J. C. H.; Doak, R. B. *Rev. Sci. Instrum.* **2012**, *83*, 035108−12.

(28) Ganan-Calvo, A. M.; Montanero, J. M. *Phys. Rev. E* **2009**, *79*, 066305.

(29) Alonso-Mori, R.; Kern, J.; Gildea, R. J.; Sokaras, D.; Weng, T.; Lassalle-Kaiser, B.; Tran, R.; Hattne, J.; Laksmono, H.; Hellmich, J.; Gloeckner, C.; Echols, N.; Sierra, R. G.; Sellberg, J.; Schafer, D. W.; Kenney, C.; Herbst, R.; Pines, J.; Hart, P.; Herrmann, S.; Grosse-Kunstleve, R. W.; Latimer, M. J.; Fry, A.; Messerschmidt, M.; Miahnahri, A.; Seibert, M. M.; Zwart, P. H.; White, W. E.; Adam, P. D.; Bogan, M. J.; Boutet, S.; Williams, G. J.; Zouni, A.; Messinger, J.; Glatzel, P.; Sauter, N. K.; Yachandra, V. K.; Yano, J.; Bergmann, U. *Proc. Natl. Acad. Sci. U.S.A.* **2012**, *109*, 19103−19107.

(30) Holton, J. M.; Frankel, K. A. *Acta Crystallogr. D* **2010**, *D66*, 393−408.

(31) Hunter, M. S.; DePonte, D. P.; Shapiro, D. A.; Kirian, R. A.; Wang, X.; Starodub, D.; Marchesini, S.; Weierstall, U.; Doak, R. B.; Spence, J. C. H.; Fromme, P. *Biophys. J.* **2011**, *100*, 198−206.

(32) Spence, J. C. H.; Kirian, R. A.; Wang, X.; Weierstall, U.; Schmidt, K. E.; White, T.; Barty, A.; Chapman, H. N.; Marchesini, S.; Holton, J. *Opt. Express* **2011**, *19*, 2866−2873.

(33) Lomb, L.; Steinbrener, J.; Bari, S.; Beisel, D.; Berndt, D.; Kieser, C.; Lukat, M.; Neef, N.; Shoeman, R. L. *J. Appl. Crystallogr.* **2012**, *45*, 674−678.

(34) Akbulut, O.; Mace, C. R.; Martinez, R. V.; Kumar, A. A.; Nie, Z.; Patton, M. R.; Whitesides, G. M. *Nano Lett.* **2012**, *12*, 4060−4064.

(35) Filipe, V.; Hawe, A.; Jiskoot, W. *Pharm. Res.* **2010**, *27*, 796−810.

(36) Kissick, D.; Gualtieri, E.; Simpson, G.; Cherezov, V. *Anal. Chem.* **2010**, *82*, 491−497.

(37) Wilson, D. J.; Konermann, L. *Anal. Chem.* **2003**, *75*, 6408−6414.

(38) Seibert, M. M.; Ekeberg, T.; Maia, F.; Svenda, M.; Andreasson, J.; Jonsson, O.; Odic, D.; Iwan, B.; Rocker, A.; Westphal, D.; Deponte, D.; Barty, A.; Schulz, J.; Gumprecht, L.; Coppola, N.; Aquila, A.; Menging, L.; White, T.; Martin, A.; Caleman, C.; Stern, S.; Abergel, C. C.; Seltzer, V.; Claverie, J. M.; Bostedt, C.; Bozek, J. D.; Boutet, S.; Miahnahri, A. A.; Messerschmidt, M.; Krzywinski, J.; Williams, G.; Hodgson, K. O.; Bogan, M. J.; Hampton, C. Y.; Sierra, R. G.; Starodub, D.; Andersson, I.; Bajt, S.; Barthelmess, M.; Spence, J. C. H.; Fromme, P.; Weierstall, U.; Kirian, R.; Hunter, M.; Doak, R. B.; Marchesini, S.; Hau-Riege, S. P.; Frank, M.; Shoeman, R. L.; Lomb, L.; Epp, S. W.; Hartman, R. L.; Rolles, D.; Rudenko, A.; Schmidt, C.; Foucar, L.; Kimmel, N.; Holl, P.; Rudek, B.; Erk, B.; Homke, A.; Reich, C.; Pietschner, D.; Weidenspointner, G.; Struder, L.; Hauser, G.; Gorke, H.; Ullrich, B.; Schlichting, I.; Herrmann, S.; Schaller, G.; Schopper, F.; Soltau, H.; Kuhnel, K. U.; Andritschke, R.; Schroter, C. D.; Krasniqi, F.; Bott, M.; Schorb, S.; Rupp, D.; Adolph, M.; Gorkhover, T.; Hirsemann, H.; Potdevin, G.; Graafsma, H.; Nilsson, B.; Chapman, H. N.; Hajdu, J. *Nature* **2011**, *470*, 78−81.

(39) Loh, N. T. D.; Hampton, C. Y.; Martin, A. V.; Starodub, D.; Sierra, R. G.; Barty, A.; Aquila, A.; Schulz, J.; Lomb, L.; Shoeman, R. L.; Kassemeyer, S.; Bostedt, C.; Bozek, J.; Epp, S.; Hartmann, R.; Rolles, D.; Rudenko, A.; Foucar, L.; Kimmel, N.; Weidenspointer, G.; Holl, P.; Pedersoli, E.; Gumprecht, L.; Liang, M.; Coppola, N.; DePonte, D. P.; Fleckenstein, H.; Hirsemann, H.; Nass, K.; White, T. A.; Tobias, H.; Barends, T.; Stier, G.; Rudek, B.; Schmidt, C.; Hoemke, A.; Hauser, G.; Farquar, G. R.; Benner, W. H.; Hau-Riege, S. P.; Reich, C.; Hartmann, A.; H., S.; Marchesini, S.; Bajt, S.; Barthelmess, M.; Kiskinova, M.; Bucksbaum, P.; Hodgson, K. O.; Strueder, L.; Ullrich, J.; Frank, M.; Schlichting, I.; Chapman, H. N.; Bogan, M. J. *Nature* **2012**, *486*, 513−517.

(40) Bogan, M. J.; Benner, W. H.; Boutet, S.; Rohner, U.; Frank, M.; Barty, A.; Seibert, M. M.; Maia, F. R. N. C.; Marchesini, S.; Bajt, S.; Woods, B. W.; Riot, V.; Hau-Riege, S. P.; Marklund, E.; Spiller, E.; Svenda, M.; Hajdu, J.; Chapman, H. N. *Nano Lett.* **2008**, *8*, 310−316.

(41) Starodub, D.; Loh, N. T. D.; Hampton, C. Y.; Sierra, R. G.; Barty, A.; Aquila, A.; Bajt, S.; Barthelmess, M.; Bostedt, C.; Bozek, J.; Coppola, N.; Epp, S.; Erk, B.; Fleckenstein, H.; Foucar, L.; Frank, M.; Graafsman, H.; Gumprecht, L.; Hartmann, A.; Hartmann, R.; Hauser, G.; Holl, P.; Kassemeyer, S.; Kimmel, N.; Liang, M.; Lomb, L.; Maia, F. R. N. C.; Marchesini, S.; Martin, A. V.; Nass, K.; Pedersoli, E.; Reich, C.; Rolles, D.; Rudek, B.; Rudenko, A.; Schulz, J.; Shoeman, R. L.; Soltau, H.; Starodub, D.; Steinbrener, J.; Stellato, F.; Strueder, L.; Ullrich, J.; Weidenspointer, G.; White, T. A.; Wunderer, C.; Spence, J. C. H.; Schlichting, I.; Chapman, H. N.; Bogan, M. J. *Nat. Commun.* **2012**, 1276.

(42) Loh, N. T. D.; Bogan, M. J.; Elser, V.; Barty, A.; Boutet, S.; Bajt, S.; Hajdu, J.; Ekeberg, T.; Maia, F. R. N. C.; Schulz, J.; Seibert, M. M.; Iwan, B.; Timneanu, N.; Marchesini, S.; Schlichting, I.; Shoeman, R.; Lomb, L.; Frank, M.; Liang, M.; Chapman, H. N. *Phys. Rev. Lett.* **2010**, *104*, 225501.

(43) Barty, A.; Kupper, J.; Chapman, H. N. *Annu. Rev. Phys. Chem.* **2013**, DOI: 10.1146/annurev-physchem-032511-143708.

(44) McCullough, B. J.; Entwistle, A.; Konishi, I.; Buffey, S.; Hasnain, S. S.; Brancia, F. L.; Grossmann, J. G.; Gaskell, S. J. *Anal. Chem.* **2009**, *81*, 3392−3397.

(45) Qizhi, H.; Robert, J. N.; Hongyan, L.; Alexander, M.; Mark, H.; Cooks, R. G. *J. Mass Spectrom.* **2005**, *40*, 430−443.

(46) Rose, R. J.; Damoc, E.; Denisov, E.; Makarov, A.; Heck, A. J. R. *Nat. Methods* **2012**, *9*, 1084−1086.

(47) Starodub, D.; Rez, P.; Hembree, G.; Howells, M.; Shapiro, D.; Chapman, H. N.; Fromme, P.; Schmidt, K.; Weierstall, U.; Doak, R. B.; Spence, J. C. H. *J. Synchrotron Rad.* **2008**, *15*, 62−73.

(48) Roberts, G. https://news.slac.stanford.edu/features/growth-spurt-x-ray-lasers, 2013.

(49) Wang, L.; Chance, M. R. *Anal. Chem.* **2011**, *83*, 7234−7241.